Biochemical Pharmacology, Vol. 41, No. 6/7, pp. 905–914, 1991.
Printed in Great Britain.

0006-2952/91 $3.00 + 0.00

FREE RADICAL PRODUCTION AND SITE-SPECIFIC DNA DAMAGE INDUCED BY HYDRALAZINE IN THE PRESENCE OF METAL IONS OR PEROXIDASE/HYDROGEN PEROXIDE

KOJI YAMAMOTO and SHOSUKE KAWANISHI*
Department of Public Health, Faculty of Medicine, Kyoto University, Kyoto 606, Japan

(*Received* 16 *August* 1990; *accepted* 23 *October* 1990)

Abstract—Hydralazine caused site-specific DNA damage in the presence of Cu(II), Co(II), Fe(III), or peroxidase/H_2O_2. The order of inducing effect of metal ions on hydralazine-dependent DNA damage [Cu(II) > Co(II) > Fe(III)] was related to that of accelerating effect on the O_2 consumption rate of hydralazine autoxidation. Catalase completely inhibited DNA damage by hydralazine plus Cu(II), but hydroxyl radical (•OH) scavengers and superoxide dismutase did not. On the other hand, DNA damage by hydralazine plus Fe(III) was inhibited by catalase and •OH scavengers. Hydralazine plus Cu(II) induced piperidine-labile sites predominantly at guanine and some adenine residues, whereas hydralazine plus Fe(III) caused cleavages at every nucleotide. Activation of hydralazine by peroxidase/H_2O_2 caused guanine-specific modification in DNA. ESR-spin trapping experiment showed that •OH and superoxide are generated during the Fe(III)- or Cu(II)-catalysed autoxidation of hydralazine, respectively, and that nitrogen-centered radical is generated during the Cu(II)- or peroxidase-catalysed oxidation. The generation of nitrogen-centered radical was also supported by HPLC–mass spectrometry. The results suggest that the guanine-specific modification by the enzymatic activation of hydralazine is due to the nitrogen-centered hydralazyl radical or derived active species, whereas •OH participates in DNA damage by hydralazine plus Fe(III). The mechanism of hydralazine plus Cu(II)-induced DNA damage is complex. The possible role of the DNA damage induced by hydralazine in the presence of Cu(II) or peroxidase/H_2O_2 is discussed in relation to hydralazine-induced lupus, mutation, and cancer.

Hydralazine, an aromatic hydrazine derivative, has been widely used in the long treatment of hypertension [1], but induces a disease with autoimmune features resembling SLE† [1, 2]. Various methods have revealed that SLE patients' sera contain antibody against DNA [3–5]. In the metabolism of hydralazine, although N-acetylation is the major metabolic pathway, *N*-acetyl derivatives have not been considered to be reactive metabolites. A main predisposing factor for hydralazine-induced SLE is slow acetylator phenotype [2].

Several hydrazine derivatives, including hydralazine, have been shown to be mutagenic and carcinogenic [6]. Two epidemiological studies suggest an association between exposure to hydralazine and incidence of cancer [7, 8], although recent study has shown no increased risk with relatively short-term use of hydralazine [9]. In 1978, Toth reported an increased incidence of lung tumors in mice treated with hydralazine [10], which has been confirmed by Drożdż *et al.* [11]. Hydralazine has been proved to be mutagenic in bacterial test systems without rat liver S-9 activation [12–15].

Regarding the molecular mechanism of hydralazine-induced SLE, mutation, and cancer, it can be speculated that hydralazine causes DNA damage by some mechanisms other than N-acetylation or S-9 activation. However, the activation mechanism remains to be clarified. We examined the induction of DNA damage by metal- or peroxidase-catalysed activation of hydralazine using ^{32}P 5′ end-labeled DNA fragments of defined sequences, and found that in the presence of Cu(II), Co(II), Fe(III), or peroxidase/H_2O_2, hydralazine causes DNA damage. The site specificity of the DNA damage was different from site specificity proposed previously by Dubroff and Reid [16]. The mechanism of the DNA damage was investigated by UV-visible, ESR and HPLC–mass spectrometries.

MATERIALS AND METHODS

Materials. Restriction enzymes (*Ava*I, *Xba*I, *Pst*I) and T_4 polynucleotide kinase were purchased from New England Biolabs. [γ-^{32}P]-ATP (6000 Ci/mmol) was from New England Nuclear (Du Pont). $CuCl_2$ and other metallic chlorides, ethanol, *tert*-butyl alcohol, and sodium formate were from Nacalai Tesque, Inc. (Kyoto, Japan). DTPA and bathocuproinedisulfonic acid were from Dojin Chemicals Co. (Kumamoto, Japan). Peroxidase (260 units/mg from horseradish) was from Toyobo Co. (Osaka, Japan). SOD (3150 units/mg from bovine erythrocytes) and catalase (45,000 units/mg from bovine liver) were from the Sigma Chemical Co. (St. Louis, MO). Hydralazine hydrochloride, phthalazine, phthalazinone, and POBN were from Aldrich Chemical Co. (Milwaukee, WI) DMPO was from Labotec Co. (Tokyo, Japan).

* To whom correspondence should be addressed.

† Abbreviations: SLE, systemic lupus erythematosus; DTPA, diethylenetriaminepentaacetic acid; SOD, superoxide dismutase; DMPO, 5,5-dimethylpyrroline-*N*-oxide; DMPO-OH, hydroxyl radical adduct of 5,5-dimethylpyrroline-*N*-oxide; POBN, α-(4-pyridyl 1-oxide)-*N*-*tert*-butylnitrone.

Preparation of ^{32}P *5′ end-labeled DNA fragments.* DNA fragments were prepared from plasmid pbcNI which carries a 6.6-kilobase *Bam*HI chromosomal DNA segment containing human c-Ha-*ras*-1 protooncogene [17, 18]. Singly labeled 261-base pair fragment (*Ava*I* 1645 - *Xba*I 1905), 341-base pair fragment (*Xba*I 1906 - *Ava*I* 2246), 98-base pair fragment (*Ava*I* 2247 - *Pst*I 2344), and 337 base-pair fragment (*Pst*I 2345 - *Ava*I* 2681) were obtained according to the method described previously [17, 18]. The asterisk indicates ^{32}P-labeling and nucleotide numbering starts with the *Bam*HI site [19].

Analysis of DNA damage induced by hydralazine. The standard reaction mixture in a microtube (1.5 mL Eppendorf) contained 0.5 mM hydralazine, metal ion or peroxidase/H_2O_2, sonicated calf thymus DNA and [^{32}P]DNA fragment in 200 μL of 10 mM sodium phosphate buffer (pH 7.9) containing 5 μM DTPA. After the incubation for the indicated duration at 37°, the DNA fragments were heated at 90° for 20 min in 1 M piperidine where indicated and treated as previously described [17, 18].

The preferred cleavage sites were determined by direct comparison of the positions of the oligonucleotides with those produced by the chemical reactions of the Maxam-Gilbert procedure [20] using a DNA sequencing system (LKB 2010 Macrophor). A laser densitometer (LKB 2222 UltroScan XL) was used for the measurement of the relative amounts of oligonucleotides from treated DNA fragments.

Measurements of UV-visible spectra and oxygen consumption during the autoxidation of hydralazine. UV-visible spectra were measured at 37° with a UV-Vis-NIR recording spectrophotometer (Shimadzu UV-365). Oxygen consumption by the autoxidation of hydralazine was measured in a thermostated (25°) water-jacketed glass vessel, fitted with a Clark electrode (Gilson) according to the method described previously [21].

ESR spectra measurements. ESR spectra were measured at room temperature using a JES-FE-3XG (JEOL, Tokyo, Japan) spectrometer with 100 kHz field modulation according to the method described previously [22, 23]. Spectra were recorded with a microwave power of 16 mW and a modulation amplitude of 1.0 or 0.4 G. The magnetic fields were calculated by the splitting of Mn(II) in MgO (ΔH_{3-4} = 86.9 G). DMPO and POBN were used as radical trapping reagents. The yield of singlet oxygen was measured by using 2,2,6,6-tetramethyl-4-piperidone [23].

HPLC-mass spectra measurements. HPLC was carried out on a LC-6A HPLC system (Shimadzu, Kyoto, Japan) using a Cosmosil 5C_{18} packed column (4.6 mm i.d. × 150 mm, Nacalai Tesque). Elution was undertaken at a flow rate of 1 mL/min with a linear gradient of acetonitrile from 10 to 50% (0 ~ 10 min) followed by 50% (10 ~ 40 min) in aqueous ammonium acetate (50 mM). Where indicated, the HPLC eluate was routed directly into a LCMS-QP1000 quadrupole mass spectrometer (Shimadzu), fitted with thermospray interface. A mass range 150–500 was scanned every 2 sec and data were acquired by an Shimadzu PAC200 data system. The ion chamber was kept at 250° and the vaporizer temperature varied between 137 and 142°.

RESULTS

Cleavages of ^{32}P*-labeled DNA fragments induced by hydralazine in the presence of metal ions or peroxidase/*H_2O_2. The extent of DNA damage was estimated by gel electrophoretic analysis. Figure 1A shows the effect of metal ions on hydralazine-dependent DNA damage. No oligonucleotide was observed with hydralazine alone (lane 2), showing that hydralazine itself is not a DNA-damaging agent. Cu(II), Co(II) and Fe(III) induced DNA damage in the presence of hydralazine (lanes 3–5), whereas Ni(II), Mn(II), Zn(II), and Cd(II) showed little or no effect under the present conditions (lanes 6–9). Metal ion alone induced little or no DNA damage. The order of ability to induce DNA damage with hydralazine was Cu(II) > Co(II) > Fe(III). DNA damage was also observed during peroxidase/H_2O_2-catalysed oxidation of hydralazine (Fig. 1B, lane 1).

Figure 2 shows the effect of concentration of hydralazine on metal ion-mediated DNA damage. In the case of Cu(II), the DNA damage was maximum at 0.5 mM hydralazine and little at 5 mM (Fig. 2A). On the other hand, the Fe(III)-mediated DNA damage increased with increasing concentration of hydralazine (Fig. 2B). The effect of concentration of hydralazine on Co(II)-mediated DNA damage was similar to that in the case of Cu(II).

Even without piperidine treatment, oligonucleotides were formed by hydralazine plus Cu(II) (Fig. 2A), Co(II) or Fe(III) (data not shown), suggesting the breakages of deoxyribose-phosphate backbone. The amounts of oligonucleotides increased with piperidine treatment in the case of Cu(II), Co(II), and Fe(III). Since altered base is readily removed from its sugar by the piperidine treatment, it is considered that the base alteration and/or liberation were induced by hydralazine plus Cu(II), Co(II) or Fe(III).

Effects of scavengers on DNA damage induced by hydralazine plus Cu(II) *or* Fe(III). Figure 3A shows the effects of SOD, catalase and hydroxyl radical (•OH) scavengers on hydralazine plus Cu(II)-induced DNA damage. Addition of •OH scavengers (ethanol, *tert*-butyl alcohol), and SOD did not inhibit DNA damage, although sodium formate inhibited it. Catalase inhibited the DNA damage, suggesting the involvement of H_2O_2. On the other hand, hydralazine plus Fe(III)-induced DNA damage was inhibited by *tert*-butyl alcohol, sodium formate, and catalase. Ethanol showed some inhibitory effect. SOD showed little effect (Fig. 3B).

Since hydralazine is supposed to be auto-oxidized to generate H_2O_2, the extent of DNA damage by hydralazine plus Cu(II) was compared with DNA damage by H_2O_2 plus Cu(II). Hydralazine plus Cu(II) caused DNA damage more efficiently than H_2O_2 plus Cu(II) (data not shown). The addition of a Cu(I)-specific chelating agent, bathocuproine, completely inhibited DNA damage by hydralazine plus Cu(II). DTPA inhibited DNA damage induced by hydralazine in the presence of Cu(II) or Fe(III)

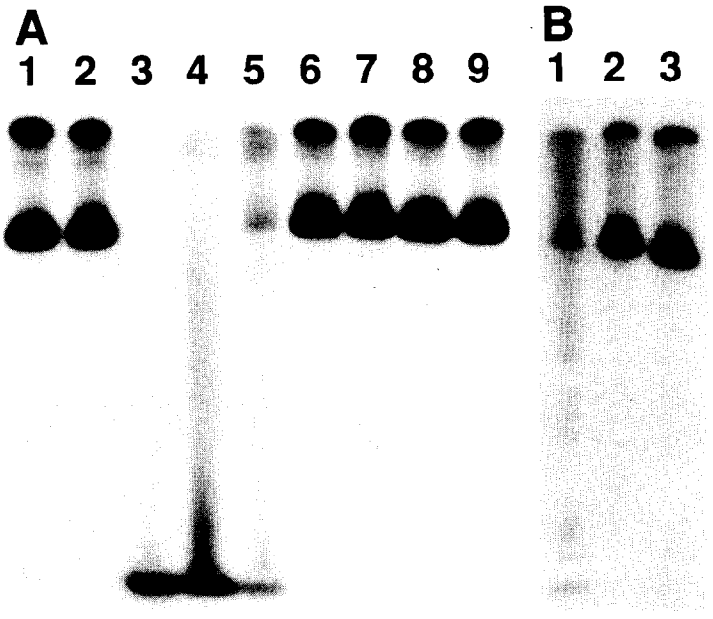

Fig. 1. Autoradiogram of ^{32}P-labeled DNA fragments incubated with hydralazine in the presence of metal ions or peroxidase/H_2O_2. (A) The reaction mixture contained the ^{32}P 5′ end-labeled 261-base pair fragment, 5 μM per base of sonicated calf thymus DNA, 0.5 mM hydralazine, metal ion, and 5 μM DTPA in 200 μL of 10 mM sodium phosphate buffer at pH 7.9. (B) The reaction mixture contained the ^{32}P 5′ end-labeled 341-base pair fragment, and 5 μM DTPA in 200 μL of 10 mM sodium phosphate buffer at pH 7.9. Where indicated, 0.5 mM hydralazine, 0.5 unit peroxidase and/or 5 mM H_2O_2 were added. After the incubation at 37° for the indicated durations, followed by the piperidine treatment, the treated DNA fragments were electrophoresed on an 8% polyacrylamide, 8 M urea gel (12 × 16 cm), and the autoradiograms were obtained by exposing X-ray film to the gel. (A) Lane 1, no metal, no hydralazine, 60 min; lane 2, no metal, 60 min; lane 3, 20 μM $CuCl_2$, 10 min; lane 4, 100 μM $CoCl_2$, 60 min; lane 5, 100 μM $FeCl_3$, 60 min lane 6, 100 μM $NiCl_2$, 60 min; lane 7, 100 μM $MnCl_2$, 60 min; lane 8, 100 μM $ZnCl_2$, 60 min; lane 9, 100 μM $CdCl_2$ 60 min. (B) Lane 1, hydralazine + peroxidase/H_2O_2; lane 2, peroxidase/H_2O_2; lane 3, hydralazine + H_2O_2.

(data not shown), indicating that metal bound to DNA is necessary for the DNA damage.

Site specificity of DNA damage induced by the metal- or peroxidase-catalysed activation of hydralazine. For the measurement of relative intensity of DNA cleavages, ^{32}P 5′ end-labeled DNA fragment incubated with hydralazine in the presence of peroxidase/H_2O_2 followed by the piperidine treatment, was electrophoresed and the autoradiogram was obtained as shown in Fig. 4. Autoradiograms were scanned with a laser densitometer (Figs 5 and 6). The DNA cleavage sites were determined by using the Maxam–Gilbert procedure [20]. In the presence of peroxidase/H_2O_2, hydralazine induced piperidine-labile sites strongly at every guanine residue (Figs 4 and 5B). Hydralazine plus Cu(II) induced piperidine-labile sites predominantly at guanine and some adenine residues (Figs 5A and 6A). The site specificity was different from that of DNA cleavage induced by H_2O_2 plus Cu(II) reported previously [17]. The DNA cleavage by hydralazine plus Fe(III) occurred at positions of every nucleotide (Fig. 6B).

Oxidation of hydralazine in the presence of metal ions or peroxidase/H_2O_2. Figure 7 shows changes in the UV-visible spectrum of hydralazine in the presence of Cu(II) with time. When Cu(II) was added to a buffer solution containing hydralazine, the absorption of hydralazine decreased. The spectral change was biphasic with the fast phase in the first 7 min followed by the slow phase. When hydralazine of the concentration smaller than that of O_2 dissolved in the air-saturated buffer was used, only the fast phase was observed. The addition of catalase prompted the autoxidation. HPLC experiment showed that hydralazine was auto-oxidized to form phthalazine (80%), phthalazinone (15%), and unknown oxidative products in the presence of Cu(II). The addition of catalase resulted in the increase of phthalazine yield and the decrease of phthalazinone yield. When peroxidase/H_2O_2 was added instead of Cu(II), hydralazine was oxidized to form phthalazine (12%), phthalazinone (6%), and several unknown oxidative products. In the presence of Fe(III), hydralazine was very slowly auto-oxidized but the oxidation products were similar to those in the case of Cu(II). One of the unknown products of Cu(II)-catalysed autoxidation showed mass spectrum with molecular ion at m/e 274 (M+1), and therefore might be identified as a dimerization product of phthalazine and 1-aminophthalazine. LaCagnin *et al.* reported that the dimerization product was also produced during the peroxidase-catalysed oxidation of hydralazine [24].

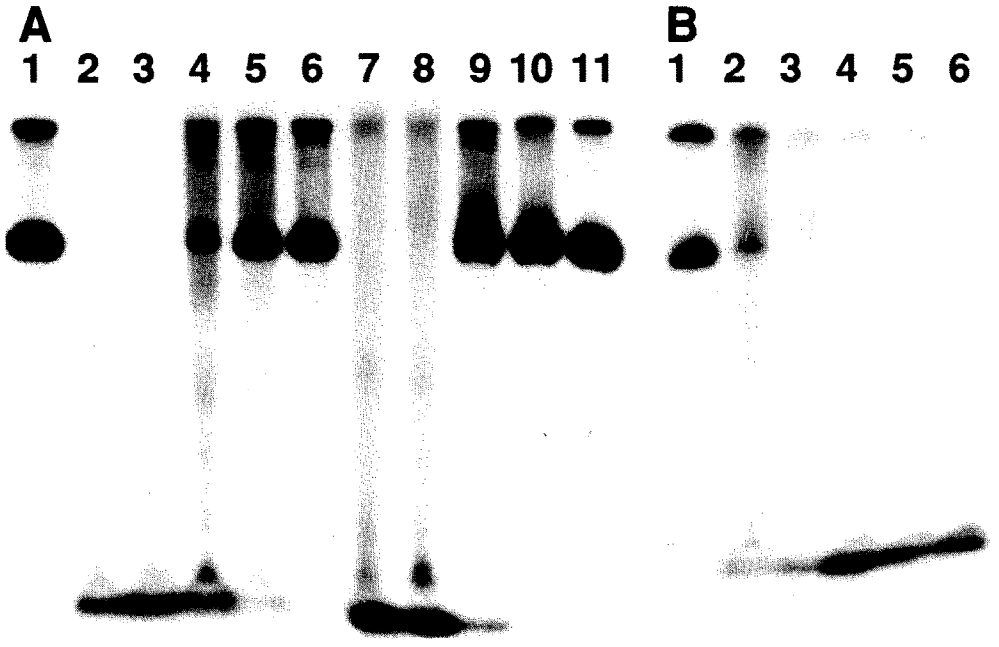

Fig. 2. DNA cleavage induced by various concentrations of hydralazine in the presence of Cu(II) or Fe(III). The reaction mixture contained the ^{32}P 5′ end-labeled 261-base pair fragment, the indicated concentration of hydralazine, metal ion, and 5 μM DTPA in 200 μL of 10 mM sodium phosphate buffer at pH 7.9. (A) 20 μM $CuCl_2$ and 25 μM per base of sonicated calf thymus DNA was added and incubated for 10 min; (B) 100 μM $FeCl_3$ and 5 μM per base of sonicated calf thymus DNA was added and incubated for 60 min. After the piperidine treatment (lanes 1–6), or without the piperidine treatment (lanes 7–11), the DNA fragments were analysed by the method described in the Fig. 1 legend. Lane 1, 0 mM; lane 2, 0.2 mM; lane 3, 0.5 mM; lane 4, 1 mM; lane 5, 2 mM: lane 6, 5 mM; lane 7, 0.2 mM; lane 8, 0.5 mM; lane 9, 1 mM; lane 10, 2 mM; lane 11, 5 mM.

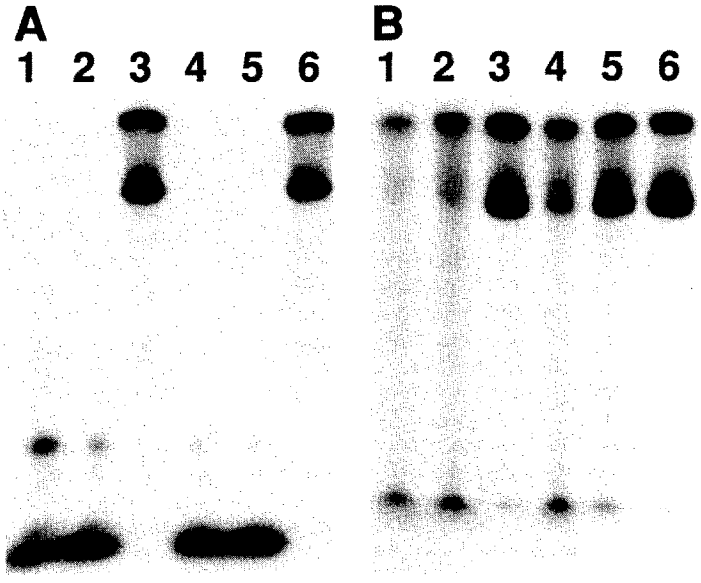

Fig. 3. Effects of SOD, catalase, and •OH scavengers on DNA cleavage induced by hydralazine in the presence of Cu(II) or Fe(III). (A) The reaction mixture contained the ^{32}P 5′ end-labeled 337-base pair fragment, 50 μM per base of sonicated calf thymus DNA, 0.5 mM hydralazine, 20 μM $CuCl_2$, scavenger, and 5 μM DTPA in 200 μL of 10 mM sodium phosphate buffer at pH 7.9. (B) The reaction mixture contained the ^{32}P5′ end-labeled 261-base pair fragment, 5 μM per base of sonicated calf thymus DNA, 0.5 mM hydralazine, 100 μM $FeCl_3$, scavenger, and 5 μM DTPA in 200 μL of 10 mM sodium phosphate buffer at pH 7.9. After the incubation at 37° for 10 min (A) or 60 min (B), followed by the piperidine treatment, the DNA fragments were analysed by the method described in the Fig. 1 legend. Lane 1, no scavenger; lane 2, 30 units of SOD; lane 3, 30 units of catalase; lane 4, 0.8 M ethanol; lane 5, 0.8 M *tert*-butyl alcohol; lane 6, 0.2 M sodium formate.

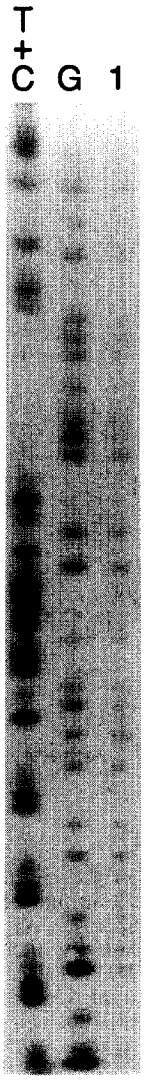

Fig. 4. Site specificity of DNA cleavage induced by hydralazine in the presence of peroxidase/H_2O_2. The ^{32}P 5′ end-labeled 337 base-pair fragment (*Pst*I 2345 - *Ava*I* 2681) in 200 μL of 10 mM sodium phosphate buffer at pH 7.9 containing 5 μM DTPA was incubated with 0.5 mM hydralazine and 0.05 unit peroxidase/2 mM H_2O_2 at 37° for 90 min. After the piperidine treatment, the DNA fragment was electrophoresed on an 8% polyacrylamide, 8 M urea gel using a DNA-sequencing system and the autoradiogram was obtained by exposing X-ray film to the gel (lane 1). The lanes T + C and G represent the patterns obtained for the same fragment after cleavage by the chemical methods of Maxam and Gilbert [20].

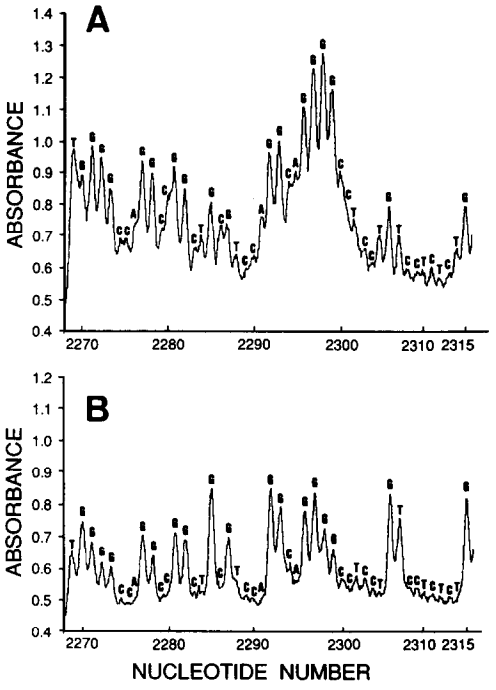

Fig. 5. Comparison of site specificity of DNA cleavage induced by hydralazine in the presence of Cu(II) and peroxidase/H_2O_2. (A) The ^{32}P 5′ end-labeled 98-base pair fragment (*Ava*I* 2247-*Pst*I 2344) in 200 μL of 10 mM sodium phosphate buffer at pH 7.9 containing 5 μM DTPA and 50 μM per base of sonicated calf thymus DNA was incubated with 0.5 mM hydralazine plus 20 μM $CuCl_2$ at 37° for 5 min. (B) The same labeled fragment and 5 μM per base of sonicated calf thymus DNA was incubated with 0.5 mM hydralazine plus 0.05 unit peroxidase/2 mM H_2O_2 at 37° for 90 min. After the piperidine treatment, DNA fragments were analysed as described in the Fig. 4 legend, and the relative amounts of oligonucleotides produced were measured by scanning the exposed X-ray film with a laser densitometer. The horizontal axis, the nucleotide number of human c-Ha-*ras*-1 protooncogene starting with the *Bam*HI site [19].

With hydralazine autoxidation, Cu(II) strongly accelerated the O_2 consumption approximately equal to hydralazine concentration. In the case of the Co(II)-catalysed autoxidation of hydralazine, O_2 consumption was biphasic with faster initial phase extending until about one-half O_2 per hydralazine was consumed. Fe(III) auto-catalytically accelerated the O_2 consumption. Ni(II) showed less effect than Fe(III). Mn(II) showed little effect. The order of catalytic ability in hydralazine autoxidation was Cu(II) > Co(II) ≫ Fe(III) > Ni(II) > Mn(II).

Production of free radicals by hydralazine in the presence of peroxidase/H_2O_2 or metal ions. Spin trapping method was used to detect free radicals produced during the autoxidation of hydralazine. Figure 8A shows that when DMPO was incubated with hydralazine in the presence of peroxidase/H_2O_2, 18 line spectrum was produced. The spin adduct (a_N = 15.0 G, $a_{H(\beta)}$ = 16.6 G, $a_{N(\beta)}$ = 2.6 G) can be assigned to the adduct of nitrogen-centered radical with DMPO by reference to the reported constants [25–27]. In order to estimate the reactivity of the nitrogen-centered hydralazyl radical with deoxyribonucleotide, the inhibitory effect of deoxyribonucleotide on the formation of the DMPO adduct was examined. Addition of dGMP and dAMP inhibited the formation of the DMPO adduct (spectra A2 and A3), and dTMP and dCMP showed less

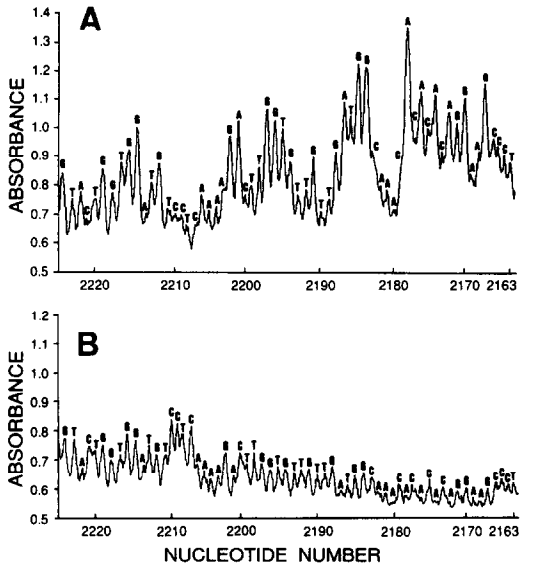

Fig. 6. Comparison of site specificity of DNA cleavage induced by hydralazine in the presence of Cu(II) and Fe(III). (A) The ^{32}P 5′ end-labeled 341-base pair fragment (*Xba*I 1906 - *Ava*I* 2246) in 200 μL of 10 mM sodium phosphate buffer at pH 7.9 containing 5 μM DTPA and 50 μM per base of sonicated calf thymus DNA was incubated with 0.5 mM hydralazine plus 20 μM $CuCl_2$ at 37° for 5 min. (B) The same labeled fragment and 5 μM per base of sonicated calf thymus DNA was incubated with 0.5 mM hydralazine plus 100 μM $FeCl_3$ at 37° for 60 min. After the piperidine treatment, DNA fragments were analysed as described in the Fig. 5 legend.

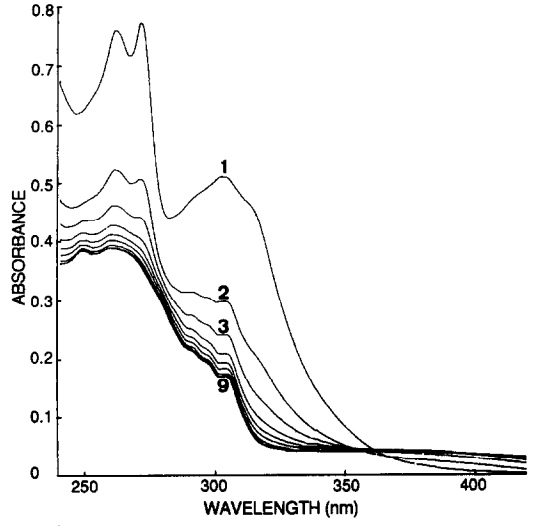

Fig. 7. Changes in UV-visible spectrum of hydralazine plus Cu(II) with time. Spectra were measured using 2 mm quartz cuvette. Sodium phosphate buffer (20 mM) at pH 7.9 containing 0.5 mM hydralazine and 5 μM DTPA was kept at 37°. After the addition of 20 μM $CuCl_2$, spectrum was measured immediately, and spectral tracing was recorded every 5 min.

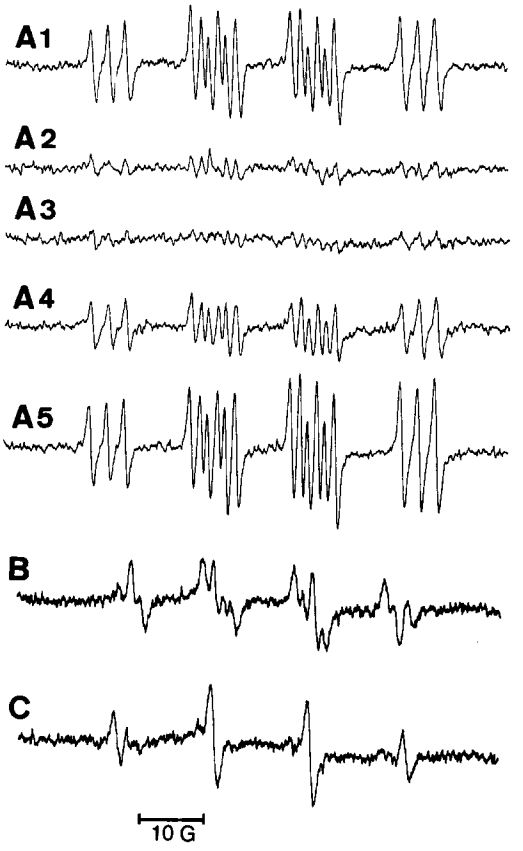

Fig. 8. ESR spectra of the radical adducts of DMPO produced by hydralazine in the presence of peroxidase/H_2O_2 or metal ions. Spectrum A1, the sample (100 μL) contained 0.5 mM hydralazine, 0.025 unit of peroxidase, 2 mM H_2O_2 and 5 μM DTPA in 50 mM sodium phosphate buffer at pH 7.9; spectrum A2, 0.1 M dGMP was added; spectrum A3, 0.1 M dAMP was added; spectrum A4, 0.1 M dTMP was added; spectrum A5, 0.1 M dCMP was added; spectrum B, the sample (100 μL) contained 2 mM hydralazine, 20 μM $CuCl_2$ and 5 μM DTPA in 20 mM sodium phosphate buffer at pH 7.9; spectrum C, the sample (100 μL) contained 2 mM hydralazine, 100 μM $FeCl_3$ and 5 μM DTPA in 20 mM sodium phosphate buffer at pH 7.9. After the addition of 146 mM DMPO followed by incubation at 25° for 5 min (A) or without incubation (B, C), aliquots of the solution were taken in a calibrated capillary, and ESR spectra were measured at room temperature as described in Materials and Methods.

inhibitory effect (spectra A4 and A5). On the other hand, when Cu(II) was added instead of peroxidase/H_2O_2, another type of signals appeared (Fig. 8B). The signals (a_N = 14.2 G, $a_{H(\beta)}$ = 11.1 G, $a_{H(\gamma)}$ = 1.3 G) can be assigned to the superoxide radical (O_2^-) adduct of DMPO [28]. Figure 8C shows an ESR spectrum of a spin adduct observed when DMPO was added to a buffer solution containing hydralazine and Fe(III). The spin adduct ($a_N = a_H$ = 14.8 G) can be reasonably assigned to DMPO-OH by reference to the reported constants [22, 23]. Catalase completely inhibited the yield of DMPO-OH.

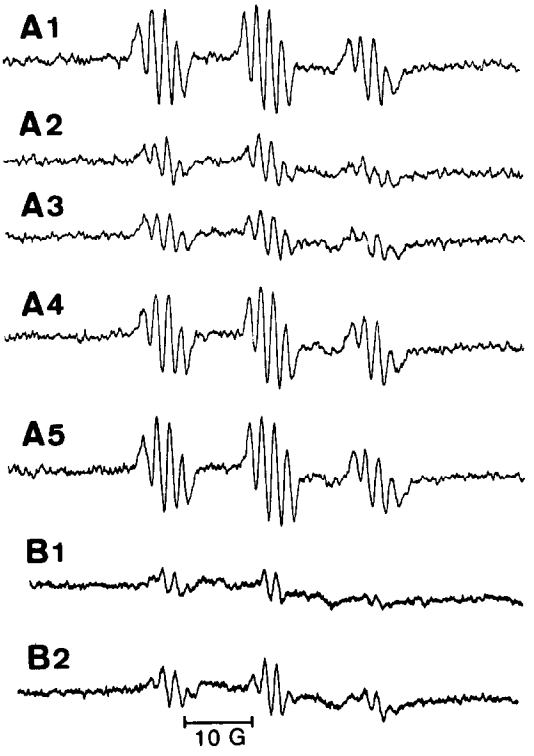

Fig. 9. ESR spectra of the radical adducts of POBN produced by hydralazine in the presence of peroxidase/H_2O_2 or Cu(II). Spectrum A1, the sample (100 μl) contained 0.5 mM hydralazine, 0.025 unit of peroxidase, 2 mM H_2O_2 and 5 μM DTPA in 20 mM sodium phosphate buffer at pH 7.9; spectrum A2, 0.1 M dGMP was added; spectrum A3, 0.1 M dAMP was added; spectrum A4, 0.1 M dTMP was added; spectrum A5, 0.1 M dCMP was added; spectrum B1, the sample (100 μL) contained 0.5 mM hydralazine, 20 μM $CuCl_2$ and 5 μM DTPA in 20 mM sodium phosphate buffer at pH 7.9; spectrum B2, 4 mM hydralazine was used instead of 0.5 mM hydralazine. After the addition of 100 mM POBN followed by incubation at 25° for 14 min (A) or immediately after the addition of 200 mM POBN (B), aliquots of the solution were taken in a calibrated capillary, and ESR spectra were measured at room temperature as described in Materials and Methods.

Figure 9A shows the 3 × 4 line ESR spectrum obtained by incubation of POBN with hydralazine in the presence of peroxidase/H_2O_2. The dominant splitting is a ^{14}N triplet ($a_N = 14.8$ G) and the secondary splittings consist of a quartet with the intensity ratio close to 1:2:2:1. The quartet is considered to originate from the combined interaction with one ^{14}N nucleus and one proton with splitting constants, $a_{N(\beta)} = a_{H(\beta)} = 1.7$ G. Incubation of hydralazine with either peroxidase or H_2O_2 produced no or little free radicals. Addition of dGMP and dAMP inhibited the formation of the POBN adduct (spectra A2 and A3), and dTMP and dCMP showed less inhibitory effects (spectra A4 and A5). When Cu(II) was added instead of peroxidase/H_2O_2, a spectrum different from that of nitrogen-centered radical appeared (spectrum B1). The formation of the spin adduct ($a_N = 14.7$ G, $a_H = 1.6$ G) was not inhibited by SOD, excluding the possibility of the adduct of O_2^-. For the present it can not be identified by reference to the reported constants [28]. When a greater amount of hydralazine was added, a mixture of nitrogen-centered radical adduct and the unidentified adduct was observed (spectrum B2).

The adduct, which was separated from the reaction mixture of POBN and hydralazine in the presence of Cu(II) by HPLC, showed mass spectrum with molecular ion at m/e 354 (M+1). The molecular ion is that expected for POBN-trapped nitrogen-centered hydralazyl radical, if a hydrogen joins in the ionization process. Another adduct of POBN showing mass spectrum with molecular ions at m/e 324 (M+1) was isolated. The molecular ion may be assigned to POBN-trapped carbon-centered phthalazinyl radical.

DISCUSSION

The present results show that hydralazine causes DNA damage in the presence of Cu(II), Co(II), or Fe(III). Neither Ni(II), Mn(II), Zn(II), nor Cd(II) showed any effect under the present conditions. Order of inducing effect on hydralazine-dependent DNA damage was Cu(II) ≫ Co(II) > Fe(III). The order was consistent with that of catalytic ability in hydralazine autoxidation. Activation of hydralazine by peroxidase/H_2O_2 also caused DNA damage. Although high concentration of hydralazine was reported to bind to and alter the tertiary structure of native DNA [29, 30], the present results show that hydralazine itself does not cause DNA damage.

In previous papers, we proposed that •OH causes cleavages at every nucleotide with a little stronger cleavages at positions of every guanine and thymine [22]. Singlet oxygen causes alteration of guanine [31]. In the case of Cu(II) plus H_2O_2-induced DNA damage, piperidine-labile sites are thymine and guanine residues [17]. The present results revealed that hydralazine plus Fe(III) caused cleavage at every nucleotide, whereas hydralazine plus Cu(II) induces piperidine-labile sites predominantly at guanine and some adenine residues. The site specificity of hydralazine plus Fe(III)-induced DNA damage can be explained by the attack by •OH. The site specificity of hydralazine plus Cu(II)-induced DNA damage cannot be explained by •OH, singlet oxygen or Cu(II) plus H_2O_2. It is noteworthy that enzymatic activation of hydralazine caused guanine-specific alteration. Although the site specificity is similar to that of DNA damage by singlet oxygen, singlet oxygen was not detected by ESR during the oxidation of hydralazine by peroxidase/H_2O_2.

In an attempt to interpret the mechanism of DNA damage induced by hydralazine in the presence of peroxidase/H_2O_2, we examined the kind of active species. ESR-spin trapping experiment showed that nitrogen-centered radical is generated during the peroxidase-catalysed oxidation of hydralazine. Therefore, it can be speculated that the nitrogen-centered hydralazyl radical causes guanine-specific modification. However, since the nitrogen-centered hydralazyl radical was shown to reactive not only to

dGMP but also to dAMP, alternative mechanism can be considered. Since it is known that benzenediazonium ion binds specifically to guanine residues in DNA [32], there remains a possibility that the diazonium ion derived from nitrogen-centered hydralazyl radical causes guanine-specific modification.

ESR-spin trapping experiments using DMPO detected •OH during the Fe(III)-catalysed autoxidation of hydralazine. DNA damage by hydralazine plus Fe(III) was inhibited by •OH scavengers. The results support the idea that hydralazine reacts with Fe(III) bound to DNA to generate •OH causing DNA damage. On the other hand, O_2^- adduct of DMPO and the adduct of nitrogen-centered hydralazyl radical with POBN were observed during the Cu(II)-catalysed autoxidation of hydralazine. Although the nitrogen-centered radical or its derived species may participate in the DNA damage especially in guanine modification, other active species can be considered. Catalase inhibited hydralazine plus Cu(II)-induced DNA damage, whereas SOD did not. The results indicate that H_2O_2 plays an important role in the production of active species causing the DNA damage and that the DNA damage is not due to O_2^-. The inhibitory effect of bathocuproine suggests that Cu(I) also plays and important role. It can be speculated that Cu(I) is produced by the reaction of Cu(II) with hydralazine. Hydralazine produces O_2^- as a consequence of the autodixation, and then the Cu(II) would rapidly react with O_2^-. This would also result in an appreciable amount of Cu(I) being present compared to Cu(II). Our previous work suggested that Cu(I) bound to DNA reacts with H_2O_2 to give ternary Cu(I)-peroxide complex which causes DNA damage [17]. Interaction of Cu(I) and DNA has been also reported by Prütz *et al.* [33]. Therefore, there arises a possibility that hydralazine intercalates to DNA and subsequently Cu(I) plus H_2O_2 reacts readily with the relaxed DNA.

On the basis of the present results we summarized a possible pathway of Cu(II)-catalysed oxidation of hydralazine as shown in Fig. 10. Phthalazine and phthalazinone have been shown to be the metabolites of hydralazine by microsomal enzymes requiring NADPH [34]. The present HPLC experiments showed that in Cu(II)-catalysed autoxidation of hydralazine, phthalazine and phthalazinone are main and minor product, respectively. The predominant yield of phthalazine can be explained by assuming that Cu(I) promotes the phthalazinyl radical formation from diazonium ion as in the case of the catalytic function of cuprous salts in Sandmeyer reaction [35]. The formation of phthalazinyl radical was suggested by HPLC-mass spectrometry. The inhibitory effect of catalase on the phthalazinone formation suggests that phthalazine is produced via carbon-centered phthalazinyl radical and that phthalazinone is formed by the reaction of phthalazinyl radical with H_2O_2. These raise a possibility that an intermediate 'X' formed by the reaction of phthalazinyl radical with H_2O_2 causes DNA damage. In the case of peroxidase-catalysed oxidation of hydralazine, the production of phthalazine and phthalazinone may be through the same

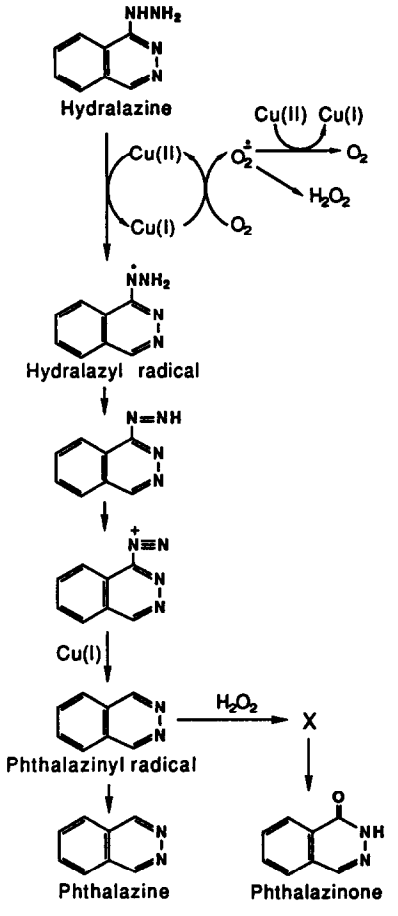

Fig. 10. A possible pathway of Cu(II)-catalysed autoxidation of hydralazine.

pathway. The unknown products of the reaction are thought to be due to the inefficiency of peroxidase in catalysing the reactions from hydralazyl radical to phthalazinyl radical and consequent side reactions. Further research is necessary to identify active species in Cu(II)- or peroxidase-catalysed hydralazine-induced DNA damage.

Regarding the molecular mechanism of hydralazine-induced SLE, mutation, and cancer, it can be speculated that the reactivity of hydralazine itself is more important than those of its metabolites. Hydralazine induced mutation in bacteria without exogenous S-9 metabolic activation system [12–15] and metabolites of hydralazine were neither genotoxic in mammalian cells nor mutagenic in bacteria [14]. In addition, McQueen *et al.* reported that DNA damage was produced by hydralazine in hepatocytes from slow acetylator rabbits but not in those from rapid acetylators [36]. Of particular interest in this regard, is the report of an increased incidence (five cases) of carcinoma in 116 patients treated with hydralazine: four of the five cases occurred in a small group of 24 patients who had developed toxic manifestations [7]. Most of the 24 patients seem to be slow acetylators [2]. It can be speculated that the metabolism of hydralazine in

slow acetylators includes mainly degradation to phthalazine through the intermediate of nitrogen-centered free radical and carbon-centered free radical. It is noteworthy that during the Cu(II)- or peroxidase-catalysed oxidation, hydralazine generates free radicals, and these free radicals or the derived active species participate in site-specific cleavage of isolated DNA. Since it was reported that copper exists in nuclei and plays a key role in determining the DNA quaternary structure [37–39], the possibility of Cu(II)-mediated hydralazine-induced DNA damage *in vivo* can be considered. On the other hand, the metabolic activation of hydralazine may be catalysed by enzymes similar to horseradish peroxidase, such as prostaglandin H synthase, since several laboratories reported that the prostaglandin H synthase can trigger metabolic activation of chemicals including carcinogens *in vitro* [40], and probably *in vivo* [41, 42]. Although whether hydralazine-induced DNA damage *in vivo* is metal- or peroxidase-mediated remains to be clarified, the DNA damage induced by the non-S-9 activation of hydralazine may be relevant for the expression of the mutagenic and carcinogenic properties of hydralazine. The fact that antibodies to chemically modified DNA is induced is of interest in relation to hydralazine-induced SLE [43, 44]. Antibodies to DNA with unusual conformation were observed in patients with SLE [45, 46]. In addition, Weisbart *et al.*, suggested a strong association between antiguanosine antibodies and the major manifestations of procainamide-induced SLE [47]. Thus, the present results led us to the idea that the hydralazine causes DNA damage by non-S-9 activation leading to the alteration of DNA conformation followed by the formation of anti-nuclear antibody.

Acknowledgements—This work was supported in part by a research grant from the Fujiwara Foundation of Kyoto University and Grant-in-Aid for Scientific Research No. 01602512 from the Ministry of Education, Science and Culture of Japan.

REFERENCES

1. Perry HM, Late toxicity to hydralazine resembling systemic lupus erythematosus or rheumatoid arthritis. *Am J Med* **54**: 58–72, 1973.
2. Mansilla-Tinoco R, Harland SJ, Ryan PJ, Bernstein RM, Dollery CT, Hughes GRV, Bulpitt CJ, Morgan A and Jones JM, Hydralazine, antinuclear antibodies, and the lupus syndrome. *Br Med J* **284**: 936–939, 1982.
3. Stollar BD and Schwartz RS, Monoclonal anti-DNA antibodies. The targets and origins of SLE autoantibodies. *Ann NY Acad Sci* **475**: 192–199, 1986.
4. Munns TW, and Freeman SK, TMP-reactive auto-antibodies in human SLE sera demonstrate thymine-dependent oligonucleotide specificity. *Biochem Biophys Res Commun* **161**: 204–210, 1989.
5. Sano H, and Morimoto C, DNA isolated from DNA/anti-DNA antibody immune complexes in systemic lupus erythematosus is rich in guanine–cytosine content. *J Immunol* **128**: 1341–1345, 1982.
6. Toth B, Actual new cancer-causing hydrazines, hydrazides, and hydrazones. *J Cancer Res Clin Oncol* **97**: 97–108, 1980.
7. Perry HM Jr, Carcinoma and hydralazine toxicity in patients with malignant hypertension. *JAMA* **186**: 1020–1022, 1963.
8. Williams RR, Feinleib M, Connor RJ and Stegens NL, Case-control study of antihypertensive and diuretic use by women with malignant and benign breast lesions detected in a mammography screening program. *J Natl Cancer Inst* **61**: 327–335, 1978.
9. Kaufman DW, Kelly JP, Rosenberg L, Stolley PD, Warshauer ME and Shapiro S, Hydralazine use in relation to cancers of the lung, colon, and rectum. *Eur J Clin Pharmacol* **36**: 259–264, 1989.
10. Toth B, Tumorigenic effect of 1-hydrazinophthalazine hydrochloride in mice. *J Natl Cancer Inst* **61**: 1363–1365, 1978.
11. Drożdż M, Luciak M, Jendryczko A and Magner K, Changes in lung activity of superoxide dismutase and copper concentration during lung tumorigenesis by hydralazine in Swiss mice. *Exp Pathol* **32**: 119–122, 1987.
12. Parodi, S, De Flora S, Cavanna, M. Pino, A, Robbiano, L. Bennicelli, C and Brambilla G. DNA-damaging activity *in vivo* and bacterial mutagenicity of sixteen hydrazine derivatives as related quantitatively to their carcinogenicity. *Cancer Res* **41**: 1469–1482, 1981.
13. Williams GM, Mazue G, McQueen CA and Shimada T, Genotoxicity of the antihypertensive drugs hydralazine and dihydralazine. *Science* **210**: 329–330, 1980.
14. Shaw CR, Butler MA, Thenot J-P, Haegle KD and Matney TS, Genetic effects of hydralazine. *Mutat Res* **68**: 79–84, 1979.
15. Tosk J, Schmeltz I and Hoffmann D, Hydrazines as mutagens in a histidine-requiring auxotroph of *Salmonella typhimurium*. *Mutat Res* **66**: 247–252, 1979.
16. Dubroff LM and Reid RJ Jr, Hydralazine-pyrimidine interactions may explain hydralazine-induced lupus erythematosus. *Science* **208**: 404–406, 1980.
17. Yamamoto K and Kawanishi S, Hydroxyl free radical is not the main active species in site-specific DNA damage induced by copper(II) ion and hydrogen peroxide. *J Biol Chem* **264**: 15435–15440, 1989.
18. Kawanishi S, Inoue S, and Kawanishi M, Human DNA damage induced by 1,2,4-benzenetriol, a benzene metabolite. *Cancer Res* **49**: 164–168, 1989.
19. Capon DJ, Chen EY, Levinson AD, Seeburg PH and Goeddel DV, Complete nucleotide sequences of the T24 human bladder carcinoma oncogene and its normal homologue. *Nature* **302**: 33–37, 1983.
20. Maxam AM and Gilbert W, Sequencing end-labeled DNA with base-specific chemical cleavages. *Methods Enzymol* **65**: 499–560, 1980.
21. Kawanishi S, Yamamoto K and Inoue S, Site-specific DNA damage induced by sulfite in the presence of cobalt(II) ion: Role of sulfate radical. *Biochem Pharmacol* **38**: 3491–3496, 1989.
22. Inoue S and Kawanishi S, Hydroxyl radical production and human DNA damage induced by ferric nitrilotriacetate and hydrogen peroxide. *Cancer Res* **47**: 6522–6527, 1987.
23. Kawanishi S, Inoue S and Sano S, Mechanism of DNA cleavage induced by sodium chromate(VI) in the presence of hydrogen peroxide. *J Biol Chem* **261**: 5952–5958, 1986.
24. LaCagnin LB, Colby HD and O'Donnell JP, The oxidative metabolism of hydralazine by rat liver microsomes. *Drug Metab Dispos* **14**: 549–554, 1986.
25. Sinha BK, Enzymatic activation of hydrazine derivatives. A spin-trapping study. *J Biol Chem* **258**: 796–801, 1983.
26. Sinha BK and Motten AG, Oxidative metabolism of hydralazine. Evidence for nitrogen centered radicals formation. *Biochem Biophys Res Commun* **105**: 1044–1051, 1982.

27. Sinha BK and Patterson MA, Free radical metabolism of hydralazine. Binding and degradation of nucleic acids. *Biochem Pharmacol* **32**: 3279–3284, 1983.
28. Buettner GR, Spin trapping: ESR parameters of spin adducts. *Free Radic Biol Med* **3**: 259–303, 1987.
29. Eldredge NT, Robertson WB and Miller JJ, The interaction of lupus-inducing drugs with deoxyribonucleic acid. *Clin Immunol Immunopathol* **3**: 263–271, 1974.
30. Tan EM, Drug-induced autoimmune disease. *Fed Proc* **33**: 1894–1897, 1974.
31. Kawanishi S, Inoue S, Sano S and Aiba H, Photodynamic guanine modification by hematoporphyrin is specific for single-stranded DNA with singlet oxygen as a mediator. *J Biol Chem* **261**: 6090–6095, 1986.
32. Stiborová M, Asfaw B, Anzenbacher P and Hodek P, A new way to carcinogenicity of azo dyes: The benzenediazonium ion formed from a non-aminoazo dye, 1-phenylazo-2-hydroxynaphthalene (Sudan I) by microsomal enzymes binds to deoxyguanosine residues of DNA. *Cancer Lett* **40**: 327–333, 1988.
33. Prütz WA, Butler J and Land EJ, Interaction of copper(I) with nucleic acids. *Int J Radiat Biol* **58**: 215–234, 1990.
34. Streeter AJ and Timbrell JA, The *in vitro* metabolism of hydralazine. *Drug Metab Dispos* **13**: 255–259, 1985.
35. Zollinger H, Reactivity and stability of arenediazonium ions. *Accounts Chem Res* **6**: 335–341, 1973.
36. McQueen CA, Maslansky CJ, Glowinski IB, Crescenzi SB, Weber WW and Williams GM, Relationship between the genetically determined acetylator phenotype and DNA damage induced by hydralazine and 2-aminofluorene in cultured rabbit hepatocytes. *Proc Natl Acad Sci USA* **79**: 1269–1272, 1982.
37. Lewis CD and Laemmli UK. Higher order metaphase chromosome structure: Evidence for metalloprotein interactions. *Cell* **29**: 171–181, 1982.
38. Bryan SE, Vizard DL, Beary DA, LaBiche RA and Hardy KJ, Partitioning of zinc and copper within subnuclear nucleoprotein particles. *Nucleic Acids Res* **9**: 5811–5823, 1981.
39. George AM, Sabovljev SA, Hart LE, Cramp WA, Harris G and Hornsey S, DNA quaternary structure in the radiation sensitivity of human lymphocytes—a proposed role of copper. *Br J Cancer* **55**: 141–144, 1987.
40. Marnett LJ, Hydroperoxide-dependent oxidations during prostaglandin biosynthesis. In: *Free Radicals in Biology* (Ed. Pryor WA), Vol. 6, pp. 63–94. Academic Press, London, 1984.
41. Boyd JA, Barrett JC and Eling TE, Prostaglandin endoperoxide synthetase-dependent cooxidation of (±)- *trans*- 7,8-dihydroxy- 7,8-dehydrobenzo(*a*)pyrene in C3H/10T½ clone 8 cells. *Cancer Res* **42**: 2628–2632, 1982.
42. Rice JR, Spry LA, Zenser TV and Davis BB, Effect of peroxidase inhibitors on an *in vivo* metabolite of the urinary bladder carcinogen *N*-[4-(5-nitro-2-furyl)-2-thiazolyl]formamide in rats. *Cancer Res* **48**: 304–309, 1988.
43. Strickland PT and Boyle JM, Immunoassay of carcinogen-modified DNA. *Prog Nucleic Acid Res Mol Biol* **31**: 1–58, 1984.
44. Blount S, Griffiths HR and Lunec J, Reactive oxygen species induce antigenic changes in DNA. *FEBS Lett* **245**: 100–104, 1989.
45. Lafer EM, Möller A, Nordheim A, Stollar BD and Rich A, Antibodies specific for left-handed Z-DNA. *Proc Natl Acad Sci USA* **78**: 3546–3550, 1981.
46. Lafer EM, Valle RPC, Möller A, Nordheim A, Schur PH, Rich A and Stollar BD, Z-DNA-specific antibodies in human systemic lupus erythematosus. *J Clin Invest* **71**: 314–321, 1983.
47. Weisbart RH, Yee WS, Colburn KK, Whang SH, Heng MK and Boucek RJ, Antiguanosine antibodies: A new marker for procainamide-induced systemic lupus erythematosus. *Ann Intern Med* **104**: 310–313, 1986.